Cell wall extensin arabinosylation is required for root directional response to salinity

Yutao Zou[1,2], Nora Gigli-Bisceglia[1], Eva van Zelm[1], Magdalena M. Julkowska[3], Yuxiao Zeng[1], Yu Cheng[1], Iko T. Koevoets[1,2], Bodil Jørgensen[4], Marcel Giesbers[5], Jelmer Vroom[5], Tijs Ketelaar[6], Bent Larsen Petersen[4], Yanxia Zhang[1*], Christa Testerink[1*]

[1]Laboratory of Plant Physiology, Wageningen University & Research
[2]Plant Cell biology, Swammerdam Institute for Life Science, Universiteit van Amsterdam
[3]Boyce Thompson Institute, Ithaca NY
[4]Department of Plant and Environmental Sciences, University of Copenhagen
[5]Wageningen Electron Microscopy Centre, Wageningen University & Research
[6]Laboratory of Cell Biology, Wageningen University & Research

*Corresponding authors: Yanxia.Zhang@wur.nl; Christa.Testerink@wur.nl

Abstract

Soil salinity is a major contributor to crop yield losses. To improve our understanding of root responses to salinity, we developed and exploit here a real-time salt-induced tilting assay (SITA). This method follows root growth upon both gravitropic and salt challenges and revealed that root bending is modulated by salinity, but not by osmotic stress. Next, this salt-specific response was measured in 345 natural Arabidopsis accessions and we discovered a genetic locus, encoding for the cell-wall modifying enzyme *Extensin Arabinose Deficient arabinosyltransferase* (ExAD), to be associated with root bending in salt. Extensins are a class of structural cell wall glycoproteins [hydroxyproline-rich glycoproteins (HRGPs)] which are post-translationally modified by O-glycosylation mostly in the form of hydroxyproline (Hyp)-arabinosylation. Here we show that salt induces ExAD-dependent Hyp-arabinosylation, influencing root bending responses and cell wall thickness. We report that *exad* mutants, which lack all cell wall Hyp-Araf_4 modifications, display increased root epidermal cell wall thickness, and are impaired in the salt- dependent root bending response. Our study thus demonstrates a requirement for extensin Hyp-arabinosylation as a novel cell wall modification for the salt-specific directional response of roots and provides new insight into the process of how plant roots sense and respond to salinity.

Key words:

Arabinosylation, Cell wall extensin, Genome-Wide Association Studies (GWAS), Root directional growth, Salinity stress

Introduction

Soil salinization is a major problem causing crop yield loss in agriculture, since most crops are sensitive to salt stress (Munns and Tester, 2008). Sodium chloride (NaCl) is the main factor causing soil salinity (FAO, 2021), affecting the plant on two levels: through osmotic stress, challenging the root water uptake, and through toxic accumulation of ions in various plant tissues (Hasegawa et al., 2000; Julkowska and Testerink, 2015). Excess of salt in soil thus obstructs various cellular processes and negatively impacts shoot and root growth (van Zelm et al., 2020). In the root, salt has been shown to modify root architecture and cell wall composition and to inhibit gravitropism (Zou et al., 2022). In response to salinity, cell wall modifications enable the increase of lignin and suberin deposition and in older tissues the formation of secondary cell walls, all contributing to limiting Na^+ entry (Voxeur et al., 2015; Karlova et al., 2021; Barberon et al., 2016; Duan et al., 2020). Moreover, salt treatment also modulates several general cell wall biosynthesis processes, such as cellulose synthesis and localization of cellulose microfibrils (Endler et al., 2015), galactan accumulation (Yan et al., 2021) and arabinose biosynthesis and metabolism (Zhao et al., 2019).

Extensins are hydroxyproline-rich glycoproteins (HRGPs) that are required for the primary cell wall architectural maintenance (Lamport et al., 2011; Liu et al., 2016). Crosslinking of extensins helps building up networks in the wall and contributes to the structural matrix (Cannon et al., 2008; Marzol et al., 2018). Extensins are post-translationally modified by hydroxylation and then subsequently by *O*-glycosylation, which includes serine-galactosylation and hydroxyproline (Hyp)-arabinosylation. In extensin Hyp-arabinosylation, several arabinosyltransferases have been identified to be involved in forming the Hyp-Ara$f_{1\text{-}4}$ side-chain at specific positions. HYDROXYPROLINE ARABINOSYLTRANSFERASES 1-3 (HPAT1-3) add the first arabinose (Hyp-Araf_1) to hydroxyprolines (Hyps) (Ogawa-Ohnishi et al., 2013) and REDUCED RESIDUAL ARABINOSE 1-3 (RRA1-3), a β-(1,2)-arabinosyltransferase adds the second arabinose residue (Hyp-Araf_2) (Velasquez et al., 2011; Egelund et al., 2007). Next, XYLOGLUCAN ENDOGLUCANASE 113 (XEG113), also a β-(1,2)-arabinosyltransferase, adds the third arabinose residue (Hyp-Araf_3) (Gille et al., 2009), and finally EXTENSIN DEFICIENT ARABINOSE (ExAD), an α-(1,3)-arabinosyltransferase, adds the fourth arabinose residue (Hyp-Araf_4) (Møller et al., 2017). Interestingly, loss of function mutants of these Hyp-arabinosylation enzymes share reduced root hair length and root hair density phenotypes

(Showalter and Basu, 2016; Petersen et al., 2021). Recent studies suggest that extensin crosslinking relies on the arabinosylation of extensin motifs, and that the cross-linked network may promote root defence to pathogen-derived elicitors and could limit colonization by pathogens (Castilleux et al., 2020). However, the role of arabinosylation in response to abiotic stress is yet unknown.

In this study, through genome wide association studies (GWAS) of root growth parameters of Arabidopsis accessions acquired by a newly developed dynamic salt-induced tilting assay (SITA), we identified a region in the Arabidopsis genome that correlated with the ability of the root to change growth direction in response to salinity. Interestingly, similar to the halotropic response (Galvan-Ampudia et al., 2013; Deolu-Ajayi et al., 2019), the salt-induced modulation of root direction in SITA is a Na^+-specific response, that does not occur in response to osmotic stress or even other monovalent cations, such as K^+. Further investigation showed a role for the *ExAD* gene, an arabinosyltransferase that adds the fourth arabinose residue to cell wall extensin Hyp-Araf_3 residues to generate Hyp-Araf_4 modified extensins. Functional analysis of loss-of-function mutants of *ExAD* lacking all Hyp-Araf$_4$ transferase activity, revealed that this process is required for the salt-specific modulation of root direction, as well as for root epidermal cell wall thickness. Moreover, Hyp-Araf$_4$ levels were found to be increased in roots treated with salt. Together, our study shows that Hyp-arabinosyation of cell wall proteins is involved in root cell wall modifications under salt stress conditions, which are required for root directional growth, revealing a crucial role of ExAD-mediated arabinosylation in root responses to salinity.

Results

Root gravitropism is modified by salt in a NaCl-specific manner

To understand the dynamics of root directional growth responses to salinity and investigate the sodium specificity of salt inhibition of gravitropism, different salts and osmotic treatments were applied in a salt-induced tilting assay (SITA) setup and dynamic root bending was recorded by a time-lapse imaging system. Four-day-old Arabidopsis Col-0 seedlings were transferred to ½ MS agar plates containing different treatments while plates were rotated 90 degrees clockwise to apply a gravistimulus, immediately followed by tracking of root growth and direction in a time-lapse system. Images were taken every 20 mins for at least 24 hours **(Figure 1A)**. After image analysis by ImageJ, Root Vector Angle (RVA) was quantified for root vector angle between the two timepoints; and Root Tip Direction (RTD) was quantified for root tip dynamic response calculated from the last 10% of the root length in the root tip **(Figure 1A)**.

Root gravitropic response was modified by NaCl compared to control conditions **(Figure 1B)**, which is consistent with previous studies (Sun et al., 2008; Dinneny et al., 2008). Interestingly, while 100 mM NaCl treatment significantly affected root tip direction away from the gravitropic direction, RTDs of seedlings transplanted to 200 mM sorbitol or 100 mM KCl were similar to those in control condition **(Figure 1B; Supplemental Video1)**. All of the treatments (NaCl, KCl or sorbitol) resulted in a reduced root growth rate when compared to control, and no significant differences were observed between NaCl, KCl and sorbitol treatments with respect to growth **(Figure 1C)**, indicating that the difference in RTD is not likely due to variations in growth rate. To assess a possible effect of root development stages, we repeated the experiments by using 3-day-old Col-0 seedlings, where similar results were observed **(Supplemental Figure S1A, B)**. We also tested the effects of right or left (anticlockwise or clockwise) 90-degree re-orientation of the plates, showing that after the initial phase, NaCl specifically modified root directional growth in both cases at later stage to a consistent right re-orientation angle **(Supplemental Fig. S1C, D)**. Furthermore, we found a dose-dependent effect of NaCl when testing a concentration range from 0 mM, 75 mM, 100 mM and 125 mM in SITA **(Figure 1D, E)**, and we selected a concentration of 100 mM NaCl treatment for an Arabidopsis natural diversity panel screen.

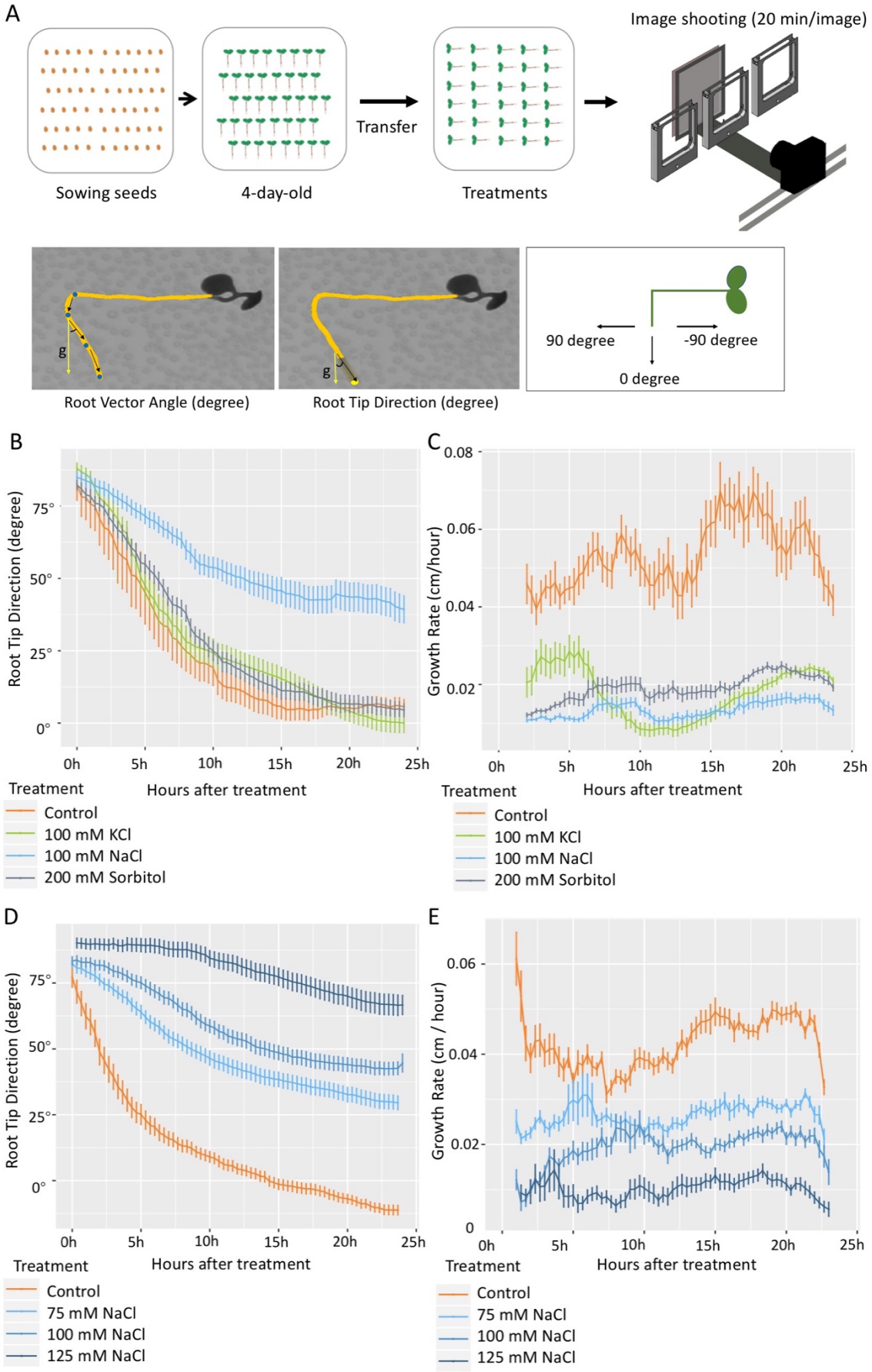
A
Image shooting (20 min/image)
Sowing seeds
4-day-old
Transfer
Treatments
g
90 degree
-90 degree
0 degree
Root Vector Angle (degree)
Root Tip Direction (degree)
B
Root Tip Direction (degree)
75°
50°
25°
0°
0h
5h
10h
15h
20h
25h
Hours after treatment
Treatment
Control
100 mM KCl
100 mM NaCl
200 mM Sorbitol
C
Growth Rate (cm/hour)
0.08
0.06
0.04
0.02
Hours after treatment
Treatment
Control
100 mM KCl
100 mM NaCl
200 mM Sorbitol
D
Root Tip Direction (degree)
Hours after treatment
Treatment
Control
75 mM NaCl
100 mM NaCl
125 mM NaCl
E
Growth Rate (cm / hour)
0.06
0.04
0.02
0
Hours after treatment
Treatment
Control
75 mM NaCl
100 mM NaCl
125 mM NaCl

Figure 1. Root Tip direction (RTD) in time-lapse SITA is specifically modulated by NaCl treatment in a dose-dependent manner. **A,** Experimental set-up of SITA. Four-day-old seedlings germinated on ½ MS medium were transferred to ½ MS agar plates containing different treatments, and at the same time plates were rotated 90 degrees anticlockwise. The root dynamic growth response was traced in a time-lapse system with an imaging frequency of one image per 20 mins for each plate. Two root angle traits were quantified as the output of image data. Root vector angle (RVA) quantified the vector angle (degree) between the two selected time-points of the roots; Root tip direction (RTD) quantified the dynamic root tip direction (degree) which showed the average direction calculated from the last 10% of the root length in the root tip. RVA and RTD are shown by the black arrow, and RTD was observed every 20 mins in time lapse while RVA was observed every 24 hrs on daily scans. Both RVA and RTD were analyzed by SmartRoot, an ImageJ plug-in for semi-automate root tracing (Lobet et al., 2011). **B** and **C**; quantification of RTD **(B)** and growth rate **(C)** of 4-day-old Col-0 seedlings under different treatments (control, 100 mM NaCl, 100 mM KCl and 200 mM sorbitol) over 24 hrs. **D** and **E**; quantification of RTD **(D)** and growth rate **(E)** of Col-0 seedlings under different concentrations of NaCl (0 mM, 75 mM, 100 mM and 125 mM) over 24 hrs. **B** and **D,** The Y-axis is RTD (degree). **C** and **E,** The Y-axis is growth rate (cm/ hour). X-axis is hours after seedlings were transferred to treatments. Values represent means ± SE from 30 seedlings, error bars represent SE of the mean. Data are representative of 3 independent experiments.

Natural variation in SITA over time and identification of candidate *loci* associated with root directional growth traits in SITA by GWAS

Given the Na^+-specificity of the SITA response, we used it as a phenotypic readout tool to identify new molecular players that underly root response to salt during gravistimulation. SITA root growth parameters were collected for 345 Arabidopsis HapMap accessions using a time-lapse system **(Table S1)**. From an initial survey performed on 20 Arabidopsis accessions **(Supplemental Figure S2)**, their root directional growth response revealed a multi-phasic response pattern during 30hrs treatment, which is described by Phase I through III. Phase I (0 hr -10 hrs) describes the acceleration stage in which the RTD of the tested accessions starts to respond to gravitropism. For most accessions, a strong effect of 100 mM NaCl on RTD was observed already during this phase, suggesting the inhibition of gravitropism by salt occurs immediately. During phase II (10 hrs – 20 hrs), most of the accessions exhibited a similar speed of directional changes under both control and NaCl conditions. In Phase III (after 20 hrs), the root growth tends to be stabilized at a final direction after the initial effects from gravitropism combined with NaCl treatment **(Supplemental Figure S2)**. Together, these results suggest that SITA can be used to monitor and quantify the NaCl-specific root phenotypic response which is a useful tool to study salt-induced root directional responses.

Root phenotypic data of the full HapMap diversity panel were subsequently analysed for correlation with SNP markers from the genome sequence of the Arabidopsis accessions (Alonso-Blanco et al., 2016) using a previously published GWAS R script, based on EMMAX and the ASReml R package (v.3.5.0) (Korte et al., 2012) and in parallel these phenotypic data were used for analysis by the online GWAPP web application (Seren et al., 2013). To map novel genetic *loci* associated with root salt stress responses, we selected three relevant traits from the SITA data to be used as input for GWAS. Identified SNPs for the early, temporal traits $K_{RTD}^{N/C}$ (response slope) and root tip direction RTD^{N-C} (RTD under NaCl –

RTD under Control) at 5 hrs **(see Supplemental Figure S3A and Table S3)** are presented in **Table S2 and S3**. Together, the natural variation data and SNPs identified for these temporal traits provide a useful resource for future investigation of early responses of roots to salt. Next, to characterize potential novel mechanisms for root directional growth responses in salt, we focused on response RVA at 23hrs (RVA^{N-C}) as a highly consistent and robust trait showing clear natural variation, and further investigated a candidate *locus* on chromosome 3 (Chr3) for this trait.

For the RVA^{N-C} at 23 hrs trait, we identified a genetic locus on chromosome 3 associated with 5 significant SNPs at or above the Bonferroni-corrected threshold on Chr3 by using the GWAPP web tool **(Figure 2A and Supplemental Table S2)**. Consistently, using the ASReml model and a panel of 4,285,827 SNPs also 5 SNPs above LOD 5.5 at the same positions were found associated with the same trait **(Supplemental Table S3)**. To study the genetic variation in the *locus*, we focused on a region that was in linkage disequilibrium with the identified SNPs, spanning approximately 16000 bp containing all the identified SNPs in the candidate locus to compare sequences of Arabidopsis HapMap accessions from the 1001 genome data base (Weigel and Mott, 2009) **(Figure 2B)**. Few regions were identified to have missing data or gaps and lower similarity in general reflected higher natural variation based on sequence alignment among all accessions compared to Col-0 **(Figure 2B, top two panels)**. Most of the low similarity peaks and significant SNPs with LOD score above the Bonferroni-corrected threshold in Chr3 are found in the *Extensin Arabinose Deficient arabinosyltransferase* (*ExAD*, AT3G57630) genomic region **(Figure 2B, lower panel)**. Next, because of the recently reported functions of cell wall modifications in salt stress responses (Zou et al., 2021) and since ExAD was previously described to function in cell wall architecture modifications, we focussed on ExAD and set out to characterize its role in regulating root directional growth in salt.

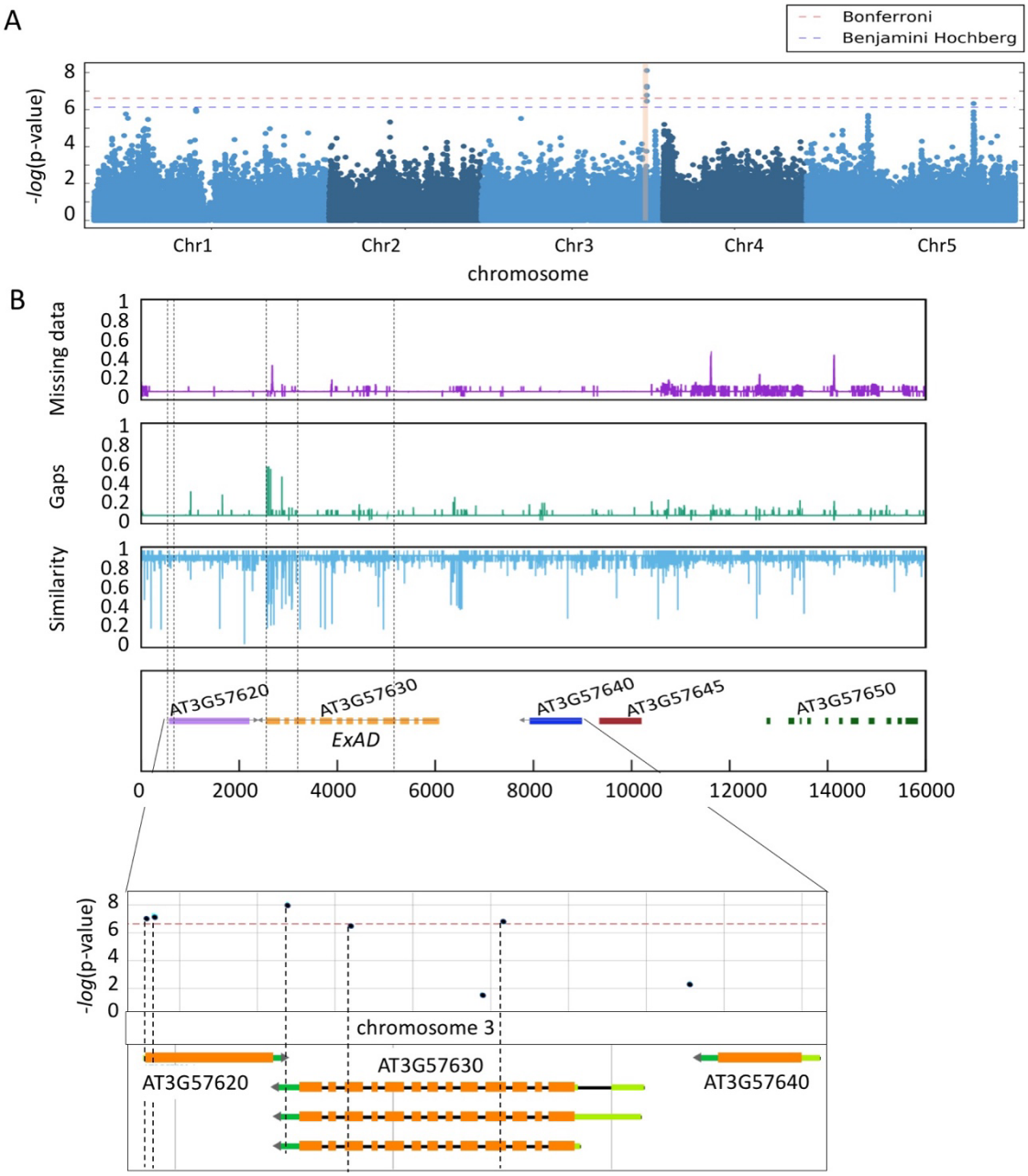

Figure 2. Natural variation in salt-modified root gravitropic response represented by root vector angle in SITA is associated with ExAD. A, Manhattan plots for the SNPs associated with response root vector angle (RVA^{N-C}) at 23hrs under salt condition subtracted by RVA under control condition. **B**, Divergence plot showing the genetic variation surrounding the significant SNPs on Chromosome 3 of all accessions in the 1001 genome database. The top purple graph represents the missing data, the middle green graph represents the gaps, and the bottom blue graph represents the similarity of SNPs compared to Col-0, respectively. Genes underlying this locus are listed in the lower panel and the location of SNPs is indicated with black dashed lines. The bottom graph zooms in the locus containing ExAD, and the location and corresponding -log10(p-value) score of the SNPs are shown accordingly using the GWAPP web application (Alonso-Blanco et al. 2016; Seren et al. 2013). The associations above the Bonferroni-corrected treshold are indicated by the red line.

Extensin Hyp-Araf$_{1-4}$ arabinosyltransferase activity is required for SITA

To investigate a possible role of extensin repeat side-chain Hyp-Araf$_{1-4}$ in regulating root growth under salt stress, first we assessed the root growth phenotypes in SITA of wild type Col-0, two *Arabidopsis* T-DNA knockout mutants *exad-1* (SAIL_843_G12), *exad-2* (SALK_204414C), and a complementation line, overexpressing *ExAD cDNA* in the *exad-1* mutant background [*hereon 35S:ExAD(exad-1)*] (Møller et al., 2017) **(Supplemental table S4)**. Four-day-old seedlings transferred to agar plates and gravistimulated with or without 100 mM NaCl, were quantified for root growth and bending after 24 hrs, 48 hrs and 72 hrs. Both *exad-1* and *exad-2* mutants showed a smaller root angle away from gravity after 24 hrs, 48 hrs and 72 hrs salt treatments compared to Col-0, but no difference in root direction was found under control condition compared with Col-0 **(Figure 3A** and **3B)**. The *35S:ExAD(exad-1)* complementation line was restored to Col-0 phenotype after 48 hrs and 72 hrs salt treatments **(Figure 3A** and **3B)**. In addition, the difference in root angle at 24 hrs, 48 hrs and 72 hrs between the tested lines is not due to differences in growth rate, since similar growth rates were observed across the lines **(Supplemental Figure S4B)**, showing that *ExAD* is specifically required for regulating root angle in SITA. Next, mutants lacking XEG113, an enzyme described to add the 3rd Ara*f* residue, which is the arabimosylation step preceding EXAD action (Gille et al., 2009) **(Figure 3C, supplementary table S4)** were tested using the same setup. Similar to the *exad* mutants, both *xeg113-1* and *xeg113-2* seedlings showed a significantly reduced root angle from the gravity vector after 24 hrs in the presence of salt **(Figure 3D and Supplemental Figure S4C)**. Together, our data suggest that ExAD and XEG113, which modify extensin repeat side-chain Hyp-Ara*f*$_3$ and Hyp-Ara*f*$_4$, respectively, are involved in regulating root directional growth in SITA. While the β-Ara*f*Ts HPAT, RRA and XEG113 have a wide selection of substrates, e.g. including the small peptide hormones (Matsubayashi, 2014) where Hyps are not extended beyond Hyp-Ara*f*$_3$, Hyp-Ara*f*$_4$ has only been found on extensins , and α-Ara*f*T ExAD is therefore considered specific to extensins (Moeller et al 2017, Petersen et al 2021). The shared phenotype of the *xeg113* and *exad* mutants thus points specifically to extensin mediated effects.

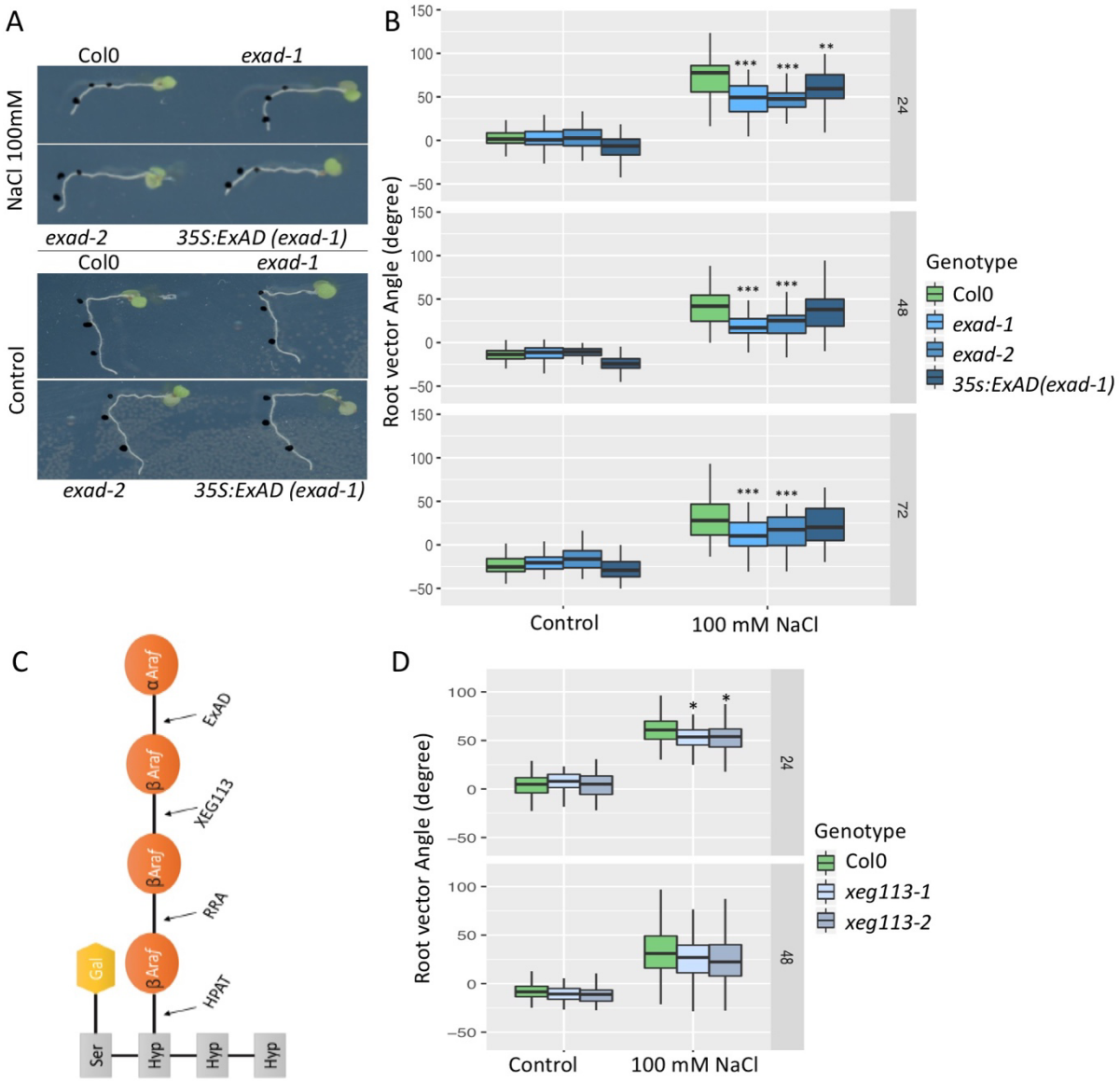

Figure 3. Extensin Hyp-Araf$_{1-4}$ arabinosyltransferase ExAD and XyG-specific endoglucanase (XEG113) are involved in modifying root vector angle and root growth rate in SITA. A Representative image of Col-0, *exad-1*, *exad-2*, and complementation line *35S: ExAD (exad-1)* in SITA. The black dots indicate the location of root tips at 0 hr, 24 hrs and 48 hrs after transferring seedlings to the treatments (with or without 100 mM NaCl). **B,** Quantification of root vector angle of Col-0, *exad-1* and *exad-2* mutants, as well as the complementation line in the *exad-1* background *35S: ExAD (exad-1)* in SITA. Four-day-old seedlings were transferred to agar plates with or without 100 mM NaCl for 24 hrs, 48 hrs and 72 hrs. Values represent means ± SE from 50 seedlings from 10 plates, each plate containing 5 seedlings. Data in (**B**) are representative of two independent experiments. **C,** Schematic diagram of extensin repeat side-chain Hyp-Ara*f*$_{1-4}$ and extensin arabinosylation enzymes. Serine is substituted with galactose and the hydroxyprolines (Hyps) are substituted with β-arabinofuranoses (β Ara*f*) and α-arabinofuranoses (α Ara*f*). HYDROXYPROLINE ARABINOSYLTRANSFERASES 1-3 (HPAT1-3) adds the first arabinose (Hyp-Ara*f*$_1$) to Hydroxyprolines (Hyps) (Ogawa-Ohnishi et al., 2013). REDUCED RESIDUAL ARABINOSE 1-3 (RRA1-3) adds the second arabinose residue (Hyp-Ara*f*$_2$) (Egelund et al., 2007; Velasquez et al., 2011). XYLOGLUCAN ENDOGLUCANASE 113 (XEG113) adds the third arabinose residue (Hyp-Ara*f*$_3$) (Gille et al., 2009). EXTENSIN DEFICIENT ARABINOSE (ExAD), as an α-(1,3)-arabinosyltransferase, ExAD adds the fourth arabinose residue (Hyp-Ara*f*$_4$) on the extensin repeat structures. **D,** Quantification of root vector angle of Col0, *xeg113-1* and *xeg113-2* mutants in SITA. Four-day-old seedlings transferred to agar plate with or without 100 mM NaCl for 24 hrs and 48 hrs. Values represent means ± SE from 7 biological replicates (plates) and 10 technical replicates (seedlings). Error bars represent SE of the mean. Statistical analysis was done using two-way ANOVA with contrasts post-hoc. Asterisks indicate statistically significant differences compared to Col0 (p-values ***P< 0.001; **P < 0.01; *P < 0.05).

Salt increases ExAD-dependent arabinosylation in Arabidopsis seedlings

To further explore effects of salt treatment on the extensin repeat side-chains Hyp-Ara*f*$_{1-4}$ and overall changes in known polysaccharides, a qualitative survey of cell wall modifications was performed using comprehensive microarray polymer profiling (CoMPP) analysis as described earlier (Moller et al., 2007). Five-day-old Col-0, *exad-1* and *exad-2* seedlings were transferred to treatments with salt (100 mM NaCl) or control (0 mM NaCl) for 2 days before harvesting for alcohol insoluble residue (AIR) extraction sequentially with CDTA and NaOH fractions, a common method for cell wall polysaccharide analysis (Fangel et al., 2021) **(**Full dataset in **Supplemental Figure S5)**. We quantified signal intensities of a selection of monoclonal antibodies (mAbs) specific to glycan epitopes **(Supplemental Table S5)**. Overall, we found that salt affects the accumulation of pectin, extensin and arabinogalactan in Col-0 and *exad-1* and *exad-2* mutants **(Supplemental Figure S5)**. A previous study suggested LM1, JIM11 and JIM20 epitopes may be specific to the third Hyp-Araf$_3$ or higher order arabinosylation of extensin repeat side-chains (Castilleux et al., 2020). However, an antibody for specific detection of Hyp-Ara*f*$_4$ has not been described. Strikingly, in this study we observed that JIM11 yielded no signal in the *exad-1* or *exad-2* mutants in either salt or control conditions, suggesting that JIM11 is specific for *ExAD*-dependent Hyp-Ara*f*$_4$ arabinosylation **(Figure 4A)**.

For polysaccharide epitope assays based on antibodies, different methods of sample preparation affect the extractability and thus may lead to variation in antibody signals (Fangel et al., 2021). Therefore, to test the robustness of JIM11 specificity and characterize further whether salt would affect the JIM11 signal in Col-0, an independent method was performed. In this case total protein was extracted, using an adapted method of (Leszczuk et al., 2020; Xu et al., 2011), from five-day-old *Arabidopsis* seedlings of Col-0 and *exad-1* mutant treated with salt (100 mM NaCl) or control for 2 days and probed for JIM11 binding on membranes **(Figure 4B)**. Consistently, no JIM11 signal was detected in the *exad-1* mutant, but a significant increase in JIM11 signal intensity was found in salt-treated Col-0 seedlings compared to control conditions **(Figure 4B)**, indicating that JIM11 specifically recognizes extensin Hyp-Ara*f*$_4$, and that salt treatment induces the Hyp-Ara*f*$_4$ levels detected by JIM11.

A

	pectin								Xyloglucan		extensin				Arabinogalactan						
	JIM5	JIM7	LM6	LM18	LM19	LM20	Inra RU1	Inra RU2	LM15	LM25	LM3	JIM11	JIM12	JIM20	LM2	LM14	JIM13	JIM16	JIM17	MAC207	
Control	56	91	23	48	66	84	41	54	7.7	12	60	35	42	33	30	40	15	17	81	21	Col-0
Control	30	27	12	51	70	0	30	33	9.3	8.7	33	0	34	28	18	22	7.4	8.4	28	9.8	*exad-1*
Control	61	81	21	58	76	61	36	43	8.7	11	61	0	48	38	27	30	9.8	15	71	15	*exad-2*
NaCl	36	40	28	44	64	0	24	27	3.6	7.3	50	36	32	35	26	32	9.6	22	35	25	Col-0
NaCl	42	56	27	48	67	29	19	18	5.5	6.5	58	0	33	33	23	26	0	12	48	20	*exad-1*
NaCl	36	30	33	58	71	0	18	17	7.2	7.7	70	0	39	38	30	30	7.7	20	30	25	*exad-2*

B

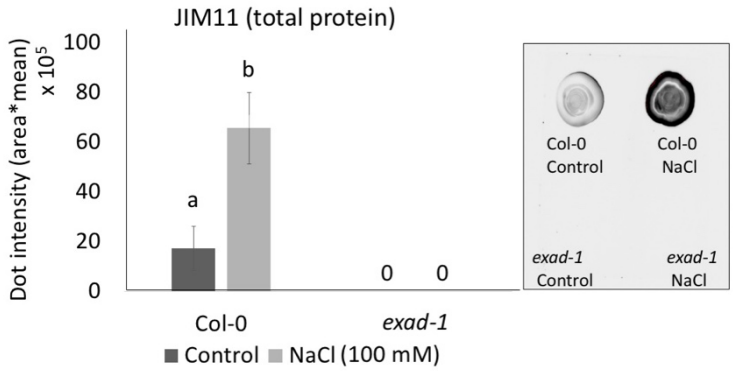

Figure 4. Anti-extensin monoclonal antibody (mAB) JIM11 is specific to ExAD-dependent arabinosylation and Hyp-Ara*f*$_4$ addition is salt-induced. A Comprehensive Microarray Polymer Profiling (CoMPP) analysis quantified mean spot intensities values (Y-axis) showing the cell-wall glycans recognized by a selection of antibodies and carbohydrate binding modules (CBMs) with CDTA extraction. Five-day-old *Arabidopsis* seedlings of Col-0 and *exad-1, exad-2* mutants were transferred to the liquid treatment medium containing control (0 mM NaCl) or salt (100 mM NaCl) for 48 hrs then harvested for cell wall alcohol-insoluble residue (AIR) extractions. A list of the antibodies used can be found in **supplemental Table S5**. Values represent means ± SE from 3 biological replicates that were isolated. Full dataset of CoMPP heatmap for all extractions (CDTA and NaOH) are shown in **Supplemental Figure S5**. **B,** antibodies JIM11 show a different pattern between *exad-1* and Col-0. Representative images and quantifications of dot-blots representative from 3 independent experiments performed with JIM11. Five-day old seedlings of Col-0 and *exad-1* mutant were transferred to the treatments with or without 100 mM NaCl for 48 hrs before harvesting. Total protein from the same weight of plant material were spotted on the nitrocellulose membrane. Statistical analysis was done using two-way ANOVA, followed with contrasts post-hoc test, different letters indicate significant differences p-value < 0.05.

ExAD is required for maintaining root cell wall thickness under salt treatment

To investigate whether ExAD-dependent arabinosylation induced by salt would affect changes in cell wall structure, we examined root epidermal cells by transmission electron microscopy (TEM). Four-day-old *Arabidopsis* seedlings of Col-0 and the *exad-1* mutant were treated with salt (100mM) for 2 days before harvesting for TEM analysis. Since the phenotype of root directional growth is due to differential cell elongation between upper and lower sides in the elongation zone (Swarup et al., 2005) and ExAD is highly expressed in the maturation zone (Møller et al., 2017), root epidermal cells in the elongation zone and maturation zone were selected for TEM. The *exad-1* mutant showed a significantly increased thickness of epidermal cell walls in both elongation and maturation zones compared to Col-

0 in sections transverse to the long axis of the root, when exposed to salt **(Figure 5).** In the elongation zone, the average thickness of the cell wall was increased in both genotypes in response to salt, with a significantly higher increase observed for *exad-1* compared to Col-0 **(Figure 5A and 5B)**. In the maturation zone, only the *exad-1* mutant showed a significantly thicker cell wall under salt conditions. No difference was observed between Col-0 and *exad-1* in control conditions **(Figure 5C and 5D)**, indicating a crucial role of *ExAD* in maintaining root cell wall thickness during salt treatment.

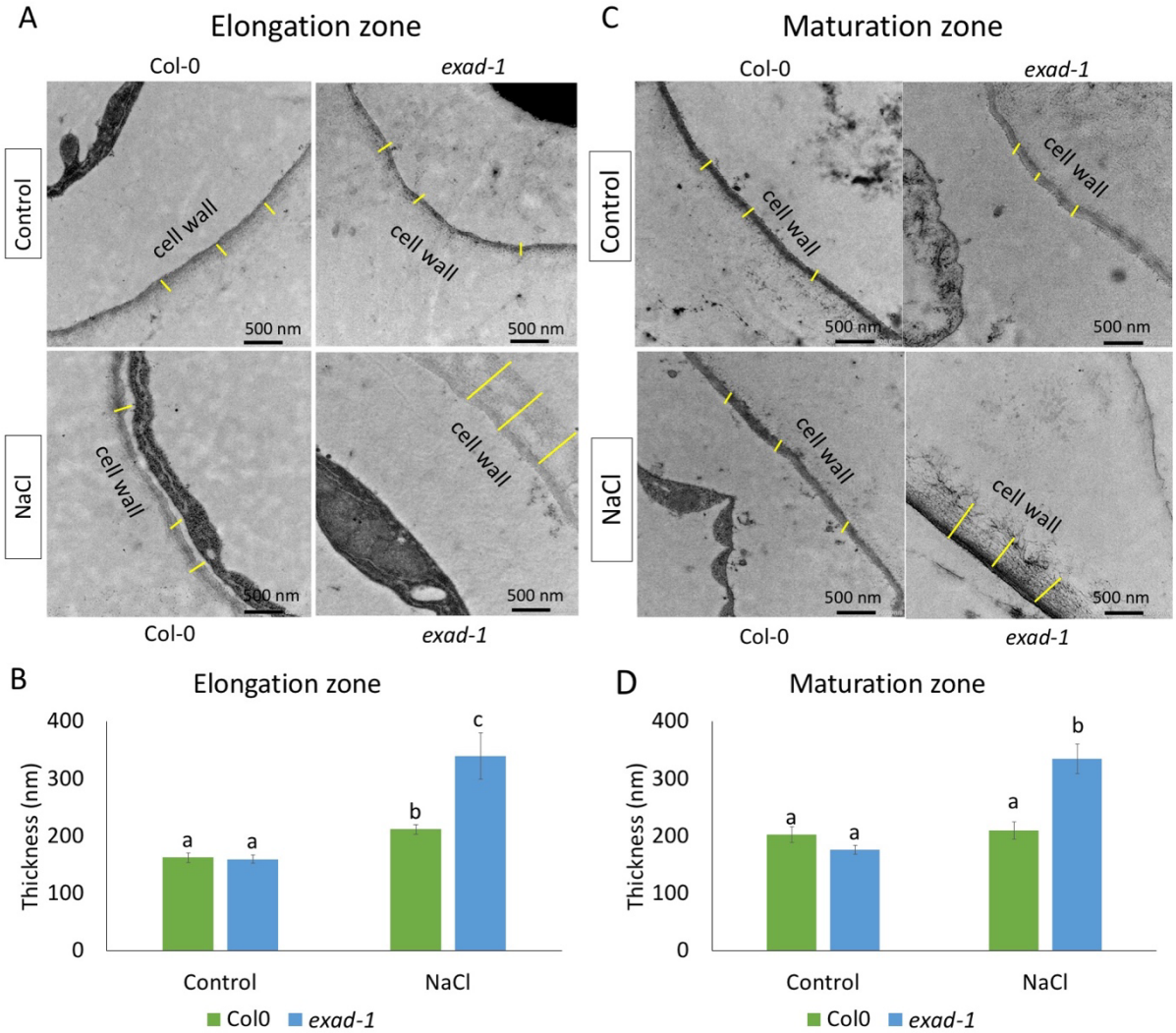

Figure 5. Transmission electron microscopy (TEM) analysis showing the involvement of ExAD in regulating root cell wall thickness under salt treatment. A-D, Cell wall structure of cells in epidermal layers in the root elongation zone **(A** and **B)**, or in the root maturation zone **(C** and **D)**. Using the SITA system, four-day-old *Arabidopsis* seedlings of Col-0 and *exad-1* mutants were transferred to the treatments with or without 100 mM NaCl for 48 hrs before sampling for TEM analysis. Representative images **(A** and **C)** and quantifications of cell wall thickness **(B** and **D)** were from 3 biological replicates, each with 3 technical replicates. Cell walls and scale bar (= 500 nm) were indicated in the images. Quantifications of cell wall thickness were measured from randomized selected 3 positions of cell wall (indicated as yellow lines) for each image. Statistical analysis was done using two-way ANOVA followed with contrasts post-hoc test, different letters indicate significant differences p-value < 0.05. Data in (**B**) and (**D**) are representative of two independent experiments.

Discussion

Salt stress negatively affects growth and development of roots in most plant species (Julkowska et al., 2014; van Zelm et al., 2020). Roots can change their growth direction dynamically to rapidly avoid a saline environment, a response that can be used as a phenotypic output to study salt signalling pathways (Deolu-Ajayi et al., 2019). In response to salt gradients, roots bend away from high salt, a process called halotropism. The mechanisms of how root halotropic responses are accomplished by redistribution of auxin have been studied in recent years (Galvan-Ampudia et al., 2013; Korver et al., 2020). On the other hand, in uniform salt conditions, little is known about the regulatory pathways and genetic components that are required for salt-induced directional growth (Sun et al., 2008). In this study, we describe a salt-induced tilting assay (SITA) to investigate root directional growth upon gravitropic challenge (gravi-stimulation) in response to salt and osmotic stress treatments. We found the SITA response could be modulated by salt, specifically Na^+ ions, but not by an equivalent level of osmotic stress **(Figure 1)**, which is similar to the halotropism response (Galvan-Ampudia et al., 2013; Deolu-Ajayi et al., 2019). We identified genetic components that may control root directional growth in SITA by using GWAS, by screening a collection of 345 natural Arabidopsis accessions. Both phenotype data and associations presented here (all raw phenotyping data available on request and to be deposited in public repository upon publication) are a useful resource for follow-up approaches to understand Na^+-specific responses of roots. Here, we focus on the characterization of one of these identified genes, coding for ExAD*,* an enzyme that modifies extensins, as a novel player in root responses mediated by cell wall modifications specifically to salinity **(Figure 2)**.

Extensins are repetitive hydroxyproline-rich O-glycoproteins (HRGPs) that have been suggested to be involved in modulating plant primary cell wall architecture (Hijazi et al., 2014). In our study, the *exad-1* mutant showed a significantly thicker cell wall structure under salt conditions **(Figure 5),** which may be linked to possible extensin cross-linking defects in the *exad-1* mutant. Well-cross-linked extensins are known to play crucial roles in supporting and maintaining cell wall architecture and cell wall formation, regulating plant growth and development, and to contribute to disease and wounding resistance (Lamport et al., 2011; Cannon et al., 2008; Lamport and Várnai, 2013). Various types of cross-links, that are built with different cell wall polymers, can be classified into homopolymeric and heteropolymeric cross-links (Mishler-Elmore et al., 2021). The heteropolymeric cross-links have been found between cell wall compositions, including pectin and cellulose (Dick-Pérez et al., 2011), pectin and extensin, pectin and hemicellulose, AGP and extensin, and extensin and lignin, as summarized earlier (Mishler-Elmore et al., 2021). Extensins can also form homopolymeric cross-links, which requires correct Hyp-arabinosylation. The extensin peroxidases *PEROXIDASE9 (PRX9)* and *PEROXIDASE40 (PRX40)* were proposed to contribute to extensin cross-linking during pollen development in Arabidopsis. (Jacobowitz et al., 2019).

Interestingly, also arabinosylation, in particular *ExAD*-dependent Hyp-α-ararabinosylation to form Hyp-Ara*f*$_4$, may be crucial for extensin crosslinking *in vitro* (Chen et al., 2015). A biotic stress study suggested that extensin arabinosylation may be involved in cell wall building and maintenance, and to protect against infection by the oomycete *P. parasitica* (Castilleux et al., 2019). Most recently, it has been hypothesized that defects in extensin arabinosylation in the Hyp-Araf mutants cause deficiency in extensin cross-linking, which may lead to cell wall architecture changes and eventually decrease plant defence resilience (Castilleux et al., 2021; Tan and Mort, 2020). Here, using TEM analysis we show the involvement of *ExAD*-dependent Hyp-~~α-~~ararabinosylation in regulating root cell wall structure under salt treatment **(Figure 5)**, which could be relevant for its role in biotic stress responses as well.

ExAD loss of function mutants were reported to have a shorter root hair phenotype (Møller et al., 2017). Interestingly, other extensin Hyp-arabinotransferase mutants showed similar phenotypes as the *exad-1* mutant. *rra* mutants (responsible for Hyp-Ara*f*$_2$) and *xeg113* mutants (responsible for Hyp-Ara*f*$_3$ formation) showed shorter root hairs (Egelund et al., 2007; Velasquez et al., 2011; Gille et al., 2009), while *hpat* mutants (responsible for Hyp-Ara*f*$_1$) were reported to have defects both in cell wall thickening and root hair elongation (Ogawa-Ohnishi et al., 2013; Velasquez et al., 2015). In our conditions in the presence of salt but not control conditions, the *exad-1* mutant had significantly thicker cell walls **(Figure 5)**. In response to salt conditions, the *exad* mutant showed a reduced response root angle of tilting away from the gravity vector compared with Col-0 under NaCl treatment **(Figure 3)**. Whether this response is linked to reduced root surface area due to shorter root hairs, which might affect salt sensitivity (Robin et al., 2016), is unclear yet.

Salt stress induces several cell wall-localized responses, such as polysaccharide deposition, changes in pectin properties and microfibril orientation, which could compromise cell wall function (Byrt et al., 2018). Recently, the cell wall has indeed been hypothesized to be crucial for salt tolerance and salt signalling pathways (Feng et al., 2018; Gigli-Bisceglia and Testerink, 2021). The *Catharanthus roseus* receptor-like kinase 1-like (CrRLK1L) protein kinase subfamily member FERONIA (FER) and the HERK1/THE1 combination have been suggested to be responsible for triggering several salt response signalling pathways, which depend on the detection of salt-induced pectin modifications (Gigli-Bisceglia et al., 2022). We now show that extensin arabinosylation is another type of cell wall modification, which is not required for root growth but for the directional response to salt stress (Figs 3 and 4). Our data suggest that extensins, being structural cell wall glycoproteins, are necessary to maintain a normal physical structure of the cell wall under stress. In the absence of Hyp-Ara*f*$_4$ extensin proteins, combined with the presence of salt, the cell wall was observed to be thicker (Figure 5). We hypothesize that this observation reflects a weaker state of the wall and we propose that extensin

arabinosylation is induced in the presence of salt, to reinforce the wall to counteract the damage done by Na^+ ions and to allow the roots to respond effectively to salinity stress.

In summary, we found that salt stress affects cell wall composition and structure in an *ExAD*-dependent way, revealing that ExAD α-ararabinosylation of extensin to yield Hyp-Araf_4 is required to build up extensin cross-linking and to modify cell wall structure during salt stress. As such, our SITA time lapse assay of root growth of a set of natural accessions in salt has revealed that cell wall modification process(es)/changes are a crucial aspect of root responses to salinity, similar to their importance for biotic stress perception (Gigli-Bisceglia and Testerink, 2021). How this process connects to other reported salt-induced cell wall modifications and how they together function in root responses and plant performance in saline conditions, remains to be established.

Material and Methods

Plant materials and growth conditions

All the seeds used in this study (listed in **Supplemental Table S1** and **Supplemental Table S4)** were propagated under long day (16 hrs light/ 8 hrs dark cycle), 21°C, 70% humidity. *Arabidopsis thaliana* seedlings of all the phenotypic assays in this study were grown under long day conditions (16hrs under white LED light/ 8hrs dark cycle), 21°C, 70% humidity. Seeds were sterilized by 30% bleach solution and stratified at 4°C for 3 days in dark before they were sown on agar plates. Seeds of mutant plants *exad-1* (SAIL_843_G12), *exad-2* (SALK_204414C) were ordered from NASC. The complementation line *35S: ExAD (exad-1)*, and *xeg113-1* (SALK_151754), *xeg113-2* (SALK_066991) were previously characterized (Møller et al., 2017). Detailed information of seeds is listed in the **Supplemental Table S4**.

For SITA, ½MS medium containing 0.1% 2(N-morpholino) ethanesulphonic acid (M.E.S.) buffer (Duchefa) and 0.5% Sucrose (Duchefa), pH5.8 adjusted with KOH, 1% Daishin agar (Duchefa) was used. For salt treatment, salt was added after adjusting PH to 5.8. In the salt specificity experiment, treatments were Control, 100 mM NaCl, 200mM Sorbitol, 100 mM KCl. In the salt dose response experiment, treatments were Control, 75, 100, 125 mM NaCl as indicated in the figure legend. In all other experiments, treatments were Control and 100 mM NaCl.

SITA

Arabidopsis thaliana seeds were dry sterilized with 40 ml thin bleach and 1.2 ml 37% HCl in a desiccator for 3 hrs, followed by at least 3 hrs in laminar flow to remove the extra surface bleach. Then

seeds were stratified in 0.1% Daishin agar solution at 4°C in the dark for 3 days before sowing. After stratification, seeds were germinated on fresh half strength (½) MS medium agar plates that were placed in 70-degree angle racks for 4 days (80 seeds per plate). Four-day-old Arabidopsis Col-0 seedlings were transferred to ½ MS agar plates containing different treatments. After transferring seedlings to treatments, all plates were rotated 90 degrees clockwise simultaneously to apply a gravi-stimulus and placed in vertical (90 degree) racks.

In the time-lapse system, all plates were captured every 20 minutes by infrared photography for at least 24 hrs. Alternatively, root tips were marked up at 24 hrs, 48 hrs and 72 hrs as indicated in figure legends.

Root phenotypic quantification and data processing

In the time-lapse system, images of plates were captured every 20 min in jpg format, at 690dpi. Alternatively, images of plates were scanned with an Epson Perfection v800 Photo scanner at 400dpi in jpg format every day. All images were improved to black/white in tiff format, and each root traced and quantified in ImageJ, SmartRoot plugin.

Two root traits were used for quantifications: Root vector angle (RVA) is measured from the beginning of the root to root tip as shown by the white arrow. Root tip direction (RTD) is indicated by the last 10% of the tracing length **(Figure 1A)**. The time-lapse system has the capacity of maximum eight plates vertically in a row and the camera (Canon 1200D) on the rail in front of plates that can move and take pictures. For each plate, the images were firstly traced manually with SmartRoot for the last time-point image, and then a SmartRoot plugin -automatic tracing- was used to trace images back at earlier time points. All the nodes during tracing were copied from the previous images to the continuous next image, and simultaneously detect the pixel intensity to remove the extra nodes from root tip. After automatic tracing, nodes in each image were inspected and adjusted manually if needed. SmartRoot was used in both time-lapse and scanning system tracing and output data into csv file, available at https://smartroot.github.io/ (Lobet et al., 2011). R was used for data and graphs processing (R scripts are available on request).

Genome Wide Association Study (GWAS)

Root SITA response traits of the HapMap accessions were collected using a time-lapse system. The phenotypic data was used in concert with SNP markers from the 1001 genome project, and Genome Wide Association Study (GWAS) was performed by two association mapping tools: GWAPP (Alonso-Blanco et al. 2016; Seren et al. 2013) and R using the EMMAX and the ASReml R package (version 3)

(Butler et al., 2009). The GWAS script included terms for correcting population structure and the kinship matrix (Korte et al., 2012). To determine population structure, PCA was performed using the factoextra R package (Kassambara and Mundt, 2017). Although the total number of SNPs encompassed 4,285,827 SNPs, only SNPs with minor allele frequency > 0.05 were considered for validation. Therefore, the Bonferroni threshold was determined by the $-\log_{10}$(p-value / # SNPs) for SNPs with minor allele frequency > 0.05. This corresponded to $-\log_{10}$ (0.05/1,753,576) = 7.55. The broadsense heritability was calculated using MVApp (Julkowska et al., 2019).

The GWAPP web application is available at http://gwapp.gmi.oeaw.ac.at/ **(Figure S5, Table S5)**. The data followed a normal distribution and the threshold for significant SNPs was determined by correcting $p < 0.1$ with Bonferroni correction. Total number of SNPs encompassed 204741 SNPs.

Sequence comparisons among accessions

Sequence information of HapMap accessions were obtained from the 1001 Genome Project (Weigel and Mott, 2009), available at http://signal.salk.edu/atg1001/3.0/gebrowser.php. Sequences were aligned with ClustalO, and the comparisons are presented in three plots including missing data, gaps and similarity by Gnu-plot software package (Julkowska et al., 2016).

T-DNA insertion line genotyping

Leaf material of 2-week-old plants was collected for DNA isolation. Tissue was grinded in liquid N2, incubated with STE/Lysis buffer (100mM Tris pH 7.5, 2% SDS, 10 mM EDTA) at 65 °C for at least 20 minutes, precipitated with Ammonium Acetate (NH4Ac). Supernatant was collected and incubated with 2-propanol and spun at a max speed. The DNA pellet was resuspended in water for PCR. Primers and SALK numbers are listed in **Table S4.**

Gene expression analysis

For gene expression analysis of *ExAD* in young seedlings, seeds were germinated on agar plates for 8 days before RNA extractions. Total RNA was extracted and purified in TRIPure (Sigma) with chloroform cleaning step, followed by DNase treatment (Ambion). cDNA was synthesized from 1 µg RNA using the reverse transcriptase - cDNA synthesis kit (Bio Rad), diluted to 10 ng/µl for qPCR with Sybr Green Supermix (Bio Rad). Reverse transcription qPCR (RT-qPCR) analysis was conducted by Bio-Rad CFX96 system. Primers used for gene expression analysis were listed in **Supplemental Table S2**.

Sequential extraction and Comprehensive Micro Array Polymer Profiling (CoMPP) analysis

Five-day-old Arabidopsis seedlings of Col-0 and *exad-1* mutant were transferred to the treatments containing (0 mM NaCl) as control, or 100 mM NaCl for 2 days before sampling. Seedling samples were harvested, flash frozen, and lyophilized. The dried material was ball milled, and the alcohol insoluble residue (AIR1) was removed by incubating the material first for 30 min in 80% ethanol, and then for 30 min in 70% ethanol at 95 °C, and finally in chloroform: methanol (1:1) for 5 min at room temperature before washing with acetone. This sequence of incubations and washes constitutes the AIR1 treatment mentioned above. Starch (AIR2) was then removed according to (Møller et al., 2017).

AIR was extracted sequentially first with 50 mM CDTA (1,2-Cyclohexylenedinitrilotetraacetic Acid) (CDTA; Merck Darmstadt, Germany) followed by 4 M NaOH, 26.5 mM NaBH4 (Merck Darmstadt, Germany). The resulting fractions (primarily pectin and hemicelluloses, respectively) was dotted on nitrocellulose using a piezoelectric array printer (Marathon, Arrayjet, Edinburgh, United Kingdom) resulting in microarrays with all the samples extractions.

The microarrays were then probed with a selection of antibodies and carbohydrate binding modules (CBMs). A list of the antibodies used can be found in **supplemental Table S2**. The microarrays were blocked with skimmed milk, probed with CBMs or monoclonal antibodies specific to glycan epitopes, and then visualized using the appropriate secondary antibodies as described in (Moller et al., 2007). Spot intensities are quantified from 256- step gray scale scans of the microarrays utilizing array detection software (Array-Pro Analyzer v 6.3, Media Cybernetics, Rockville, Maryland, United States) and data are presented on a relative scale with 100 assigned to the most intense spot. The extracted CoMPP fractions were dialyzed against demineralized water using Visking® 12-14 kDa dialysis tubing (45 mm) prior to determination of the monosaccharide composition.

JIM11 dot blot assay

4-day-old seedlings were transferred to treatments of control or NaCl (100 mM) for 48 hrs before harvesting. Samples were frozen, ground into a fine powder with a paint shaker. At least 3 biological replicates for each treatment and each genotype were used. Total protein was extracted in buffer: 0,5 M Tris-HCl (pH 6.8), 0.037 g/L EDTA (Na_2 EDTA•$2H_2O$), 2% SDS. Similar weight of samples and buffer were added/mixed with concentration 1 g/ml. 30 µl of samples were boiled at 98 °C for 3 mins. After a short centrifuge (15 mins, 13.000 xg), supernatants were collected. 20 µl of total proteins were spotted on nitrocellulose membrane. Membranes were dried at least for 4 hrs at 4 °C. Blocking (5% BSA in s) was performed for 1 h. Membranes were incubated for 1 hr with primary antibody JIM11 (Agrisera) in (1:500 in 5% BSA powder in 1×TBST). Membranes were incubated with secondary antibodies rat (IgG)

(1: 6000 in 5% milk PBS) and after washing chemiluminescence induced with Clarity Western ECL Substrate (BIO-RAD) and detected with ChemiDoc imaging system (Biorad).

Transmission electron microscopy (TEM)

Four-day-old seedlings were transferred to treatment agar plates supplemented with 100mM NaCl or 0mM as control for 48 hrs before sampling in SITA system. Specimen was cut into small pieces of about $1mm^3$ at the selected zones (elongation zone and maturation zone) before fixation. Root pieces were submerged and incubated with (2.5% glutaralehyde + 2% paraformaldehyde in 0.1M phosphate/citrate) buffer for at least 1 hour at room temperature. Specimen was washed at least 6 times for 10 mins in 0.1M phosphate/citrate buffer (washing buffer). 1% osmium tetroxide in 0.1M phosphate/citrate buffer was added and incubated for 1 hour at room temperature. Specimen was washed at 3 times for 10 minutes in MQ. Next, specimen was dehydrated in a graded ethanol series: 30% for 5 mins, 50% for 5 mins, 70% for 5 mins, 80% for 5 mins, 90% for 5 mins, 96% for 5 mins, 100% for 10 mins, and infiltrated with resin (spurr's resin) 1:2 resin:ethanol for 30 mins, 1:1 resin:ethanol for 30 mins, 2:1 resin:ethanol for 30 mins, 100% resin for 60 mins or overnight at room temperature. Leica EM Rapid was used for trimming (pre-sectioning) of the sample and Leica Ultramicrotome U7 was used for sectioning and attaining the sections. Sections were viewed using a JEOL 1400 TEM operating at 120 kV.

Statistical analysis

Statistical analysis in this study was performed in R. The normal distributions of phenotypic data were fitted in a linear model and two-way ANOVA was performed followed with contrasts post-hoc test. Treatments and genotypes were selected as the factors, and post-hoc contrasts comparison was performed with the ghlt (multcomp) package. For comparison between two groups, a T-test was performed.

Acknowledgements

We thank Leónie Bentsink and Leo Willems of the Seed lab, Laboratory of Plant Physiology, Wageningen University & Research for providing HapMap seeds for the GWAS screen. Yutao Zou is sponsored by the China Scholarship Council (CSC), Christa Testerink acknowledges support from the European Research Council (ERC); Y. Zhang and C. Testerink are funded through the European Union's Horizon 2020 Research and Innovation program (ERC Consolidator Grant agreement 724321).

Author Contributions

C.T. conceived the project, C.T., Yx.Z and Yut.Z designed experiments and wrote the manuscript. C.T and Yx.Z guided the research. Yut.Z performed most of the experiments. N.G.B guided the dot-blot experiments. E.Z. provided scripts for root slope analysis. M.M.J performed and interpreted GWAS analysis. Yux.Z and Y.C. performed the tilting assay for *exad-1* and *xeg113* mutants. I.T.K provided scripts for root angle analysis. B.J and B.L.P performed CoMPP analysis. M.G, J.V, and T.K guided and performed TEM imaging. All authors commented on and approved the manuscript.

Competing Interests

The authors declare that there is no conflict of interest.

References

Alonso-Blanco, C. et al. (2016). 1,135 Genomes Reveal the Global Pattern of Polymorphism in Arabidopsis thaliana. Cell 166: 481–491.

Barberon, M., Vermeer, J.E.M., De Bellis, D., Wang, P., Naseer, S., Andersen, T.G., Humbel, B.M., Nawrath, C., Takano, J., Salt, D.E., and Geldner, N. (2016). Adaptation of Root Function by Nutrient-Induced Plasticity of Endodermal Differentiation. Cell 164: 447–459.

Byrt, C.S., Munns, R., Burton, R.A., Gilliham, M., and Wege, S. (2018). Root cell wall solutions for crop plants in saline soils. Plant Sci. 269: 47–55.

Cannon, M.C., Terneus, K., Hall, Q., Tan, L., Wang, Y., Wegenhart, B.L., Chen, L., Lamport, D.T.A., Chen, Y., and Kieliszewski, M.J. (2008). Self-assembly of the plant cell wall requires an extensin scaffold. Proc. Natl. Acad. Sci. U. S. A. 105: 2226–2231.

Castilleux, R., Plancot, B., Gügi, B., Attard, A., Loutelier-Bourhis, C., Lefranc, B., Nguema-Ona, E., Arkoun, M., Yvin, J.-C., Driouich, A., and Vicré, M. (2020). Extensin arabinosylation is involved in root response to elicitors and limits oomycete colonization. Ann. Bot. 125: 751–763.

Castilleux, R., Plancot, B., Gügi, B., Attard, A., Loutelier-Bourhis, C., Lefranc, B., Nguema-Ona, E., Arkoun, M., Yvin, J.-C., Driouich, A., and Vicré, M. (2019). Extensin arabinosylation is involved in root response to elicitors and limits oomycete colonization. Ann. Bot. 22: 1–13.

Castilleux, R., Plancot, B., Vicré, M., Nguema-Ona, E., and Driouich, A. (2021). Extensin, an underestimated key component of cell wall defence? Ann. Bot. 127: 709–713.

Chen, Y., Dong, W., Tan, L., Held, M.A., and Kieliszewski, M.J. (2015). Arabinosylation Plays a Crucial Role in Extensin Cross-linking In Vitro . Biochem. Insights 8s2: BCI.S31353.

Deolu-Ajayi, A.O., Meyer, A.J., Haring, M.A., Julkowska, M.M., and Testerink, C. (2019). Genetic Loci Associated with Early Salt Stress Responses of Roots. iScience 21: 458–473.

Dick-Pérez, M., Zhang, Y., Hayes, J., Salazar, A., Zabotina, O.A., and Hong, M. (2011). Structure and interactions of plant cell-wall polysaccharides by two- and three-dimensional magic-angle-spinning solid-state NMR. Biochemistry 50: 989–1000.

Dinneny, J.R., Long, T.A., Wang, J.Y., Jung, J.W., Mace, D., Pointer, S., Barron, C., Brady, S.M., Schiefelbein, J., and Benfey, P.N. (2008). Cell identity mediates the response of Arabidopsis roots to abiotic stress. Science (80-.). 320: 942–945.

Duan, A.Q., Tao, J.P., Jia, L.L., Tan, G.F., Liu, J.X., Li, T., Chen, L.Z., Su, X.J., Feng, K., Xu, Z.S., and Xiong, A.S. (2020). AgNAC1, a celery transcription factor, related to regulation on lignin biosynthesis and salt tolerance. Genomics 112: 5254–5264.

Egelund, J., Obel, N., Ulvskov, P., Geshi, N., Pauly, M., Bacic, A., and Petersen, B.L. (2007). Molecular characterization of two Arabidopsis thaliana glycosyltransferase mutants, rra1 and rra2, which have a reduced residual arabinose content in a polymer tightly associated with the cellulosic wall residue. Plant Mol. Biol. 64: 439–451.

Endler, A., Kesten, C., Schneider, R., Zhang, Y., Ivakov, A., Froehlich, A., Funke, N., and Persson, S. (2015). A Mechanism for Sustained Cellulose Synthesis during Salt Stress. Cell 162: 1353–1364.

Fangel, J.U., Jones, C.Y., Ulvskov, P., Harholt, J., and Willats, W.G.T. (2021). Analytical implications of different methods for preparing plant cell wall material. Carbohydr. Polym. 261: 117866.

FAO (2021). Global map of salt-affected soils.

Feng, W. et al. (2018). The FERONIA Receptor Kinase Maintains Cell-Wall Integrity during Salt Stress through Ca2+ Signaling. Curr. Biol. 28: 666-675.e5.

Galvan-Ampudia, C.S., Julkowska, M.M., Darwish, E., Gandullo, J., Korver, R.A., Brunoud, G., Haring, M.A., Munnik, T., Vernoux, T., and Testerink, C. (2013). Halotropism is a response of plant roots to avoid a saline environment. Curr. Biol. 23: 2044–2050.

Gigli-Bisceglia, N. and Testerink, C. (2021). Fighting salt or enemies: shared perception and signaling strategies. Curr. Opin. Plant Biol. 64: 102120.

Gigli-Bisceglia, N., van Zelm, E., Huo, W., Lamers, J., and Testerink, C. (2022). Arabidopsis root responses to salinity depend on pectin modification and cell wall sensing. Development: 2020.12.18.423458.

Gille, S., Hänsel, U., Ziemann, M., and Pauly, M. (2009). Identification of plant cell wall mutants by means of a forward chemical genetic approach using hydrolases. Proc. Natl. Acad. Sci. U. S. A. 106: 14699–14704.

Hasegawa, P.M., Bressan, R.A., Zhu, J.-K., and Bohnert, H.J. (2000). PLANT CELLULAR AND MOLECULAR RESPONSES TO HIGH SALINITY. Annu. Rev. Plant Physiol. Plant Mol. Biol. 51: 463–499.

Hijazi, M., Velasquez, S.M., Jamet, E., Estevez, J.M., and Albenne, C. (2014). An update on post-translational modifications of

hydroxyproline-rich glycoproteins: Toward a model highlighting their contribution to plant cell wall architecture. Front. Plant Sci. 5: 1–10.

Jacobowitz, J.R., Doyle, W.C., and Weng, J.K. (2019). PRX9 and PRX40 are extensin peroxidases essential for maintaining tapetum and microspore cell wall integrity during arabidopsis anther development. Plant Cell 31: 848–861.

Julkowska, M.M., Hoefsloot, H.C.J., Mol, S., Feron, R., De Boer, G.J., Haring, M.A., and Testerink, C. (2014). Capturing arabidopsis root architecture dynamics with root-fit reveals diversity in responses to salinity. Plant Physiol. 166: 1387–1402.

Julkowska, M.M., Klei, K., Fokkens, L., Haring, M.A., Schranz, M.E., and Testerink, C. (2016). Natural variation in rosette size under salt stress conditions corresponds to developmental differences between Arabidopsis accessions and allelic variation in the LRR-KISS gene. J. Exp. Bot. 67: 2127–2138.

Julkowska, M.M., Saade, S., Agarwal, G., Gao, G., Pailles, Y., Morton, M., Awlia, M., and Tester, M. (2019). MV app-multivariate analysis application for streamlined data analysis and curation. Plant Physiol. 180: 1261–1276.

Julkowska, M.M. and Testerink, C. (2015). Tuning plant signaling and growth to survive salt. Trends Plant Sci. 20: 586–594.

Karlova, R., Boer, D., Hayes, S., and Testerink, C. (2021). Root plasticity under abiotic stress. Plant Physiol.: 1–14.

Korte, A., Vilhjálmsson, B.J., Segura, V., Platt, A., Long, Q., and Nordborg, M. (2012). A mixed-model approach for genome-wide association studies of correlated traits in structured populations. Nat. Genet. 44: 1066–1071.

Korver, R.A., van den Berg, T., Meyer, A.J., Galvan-Ampudia, C.S., ten Tusscher, K.H.W.J., and Testerink, C. (2020). Halotropism requires phospholipase Dζ1-mediated modulation of cellular polarity of auxin transport carriers. Plant Cell Environ. 43: 143–158.

Lamport, D.T.A., Kieliszewski, M.J., Chen, Y., and Cannon, M.C. (2011). Role of the Extensin Superfamily in Primary Cell Wall Architecture. Plant Physiol. 156: 11–19.

Lamport, D.T.A. and Várnai, P. (2013). Periplasmic arabinogalactan glycoproteins act as a calcium capacitor that regulates plant growth and development. New Phytol. 197: 58–64.

Leszczuk, A., Zając, A., Kurzyna-Szklarek, M., Cybulska, J., and Zdunek, A. (2020). Investigations of changes in the arabinogalactan proteins (AGPs) structure, size and composition during the fruit ripening process. Sci. Rep. 10: 1–14.

Liu, X., Wolfe, R., Welch, L.R., Domozych, D.S., Popper, Z.A., and Showalter, A.M. (2016). Bioinformatic identification and analysis of extensins in the plant kingdom. PLoS One 11: 1–21.

Lobet, G., Pagès, L., and Draye, X. (2011). A novel image-analysis toolbox enabling quantitative analysis of root system architecture. Plant Physiol. 157: 29–39.

Marzol, E., Borassi, C., Bringas, M., Sede, A., Rodríguez Garcia, D.R., Capece, L., and Estevez, J.M. (2018). Filling the Gaps to Solve the Extensin Puzzle. Mol. Plant 11: 645–658.

Matsubayashi, Y. (2014). Posttranslationally modified small-peptide signals in plants. Annu. Rev. Plant Biol. 65: 385–413.

Mishler-Elmore, J.W., Zhou, Y., Sukul, A., Oblak, M., Tan, L., Faik, A., and Held, M.A. (2021). Extensins: Self-Assembly, Crosslinking, and the Role of Peroxidases. Front. Plant Sci. 12.

Moller, I., Sørensen, I., Bernal, A.J., Blaukopf, C., Lee, K., Øbro, J., Pettolino, F., Roberts, A., Mikkelsen, J.D., Knox, J.P., Bacic, A., and Willats, W.G.T. (2007). High-throughput mapping of cell-wall polymers within and between plants using novel microarrays. Plant J. 50: 1118–1128.

Møller, S.R. et al. (2017). Identification and evolution of a plant cell wall specific glycoprotein glycosyl transferase, ExAD. Sci. Rep. 7: 1–16.

Munns, R. and Tester, M. (2008). Mechanisms of Salinity Tolerance. Annu. Rev. Plant Biol. 59: 651–681.

Ogawa-Ohnishi, M., Matsushita, W., and Matsubayashi, Y. (2013). Identification of three hydroxyproline O-arabinosyltransferases in Arabidopsis thaliana. Nat. Chem. Biol. 9: 726–730.

Petersen, B.L., MacAlister, C.A., and Ulvskov, P. (2021). Plant Protein O-Arabinosylation. Front. Plant Sci. 12.

Robin, A.H.K., Matthew, C., Uddin, M.J., and Bayazid, K.N. (2016). Salinity-induced reduction in root surface area and changes in major root and shoot traits at the phytomer level in wheat. J. Exp. Bot. 67: 3719–3729.

Seren, Ü., Vilhjálmsson, B.J., Horton, M.W., Meng, D., Forai, P., Huang, Y.S., Long, Q., Segura, V., and Nordborg, M. (2013). GWAPP: A web application for genome-Wide association mapping in arabidopsis. Plant Cell 24: 4793–4805.

Showalter, A.M. and Basu, D. (2016). Extensin and arabinogalactan-protein biosynthesis: Glycosyltransferases, research challenges, and biosensors. Front. Plant Sci. 7.

Sun, F., Zhang, W., Hu, H., Li, B., Wang, Y., Zhao, Y., Li, K., Liu, M., and Li, X. (2008). Salt modulates gravity signaling pathway to regulate growth direction of primary roots in arabidopsis. Plant Physiol. 146: 178–188.

Swarup, R., Kramer, E.M., Perry, P., Knox, K., Leyser, H.M.O., Haseloff, J., Beemster, G.T.S., Bhalerao, R., and Bennett, M.J. (2005). Root

gravitropism requires lateral root cap and epidermal cells for transport and response to a mobile auxin signal. Nat. Cell Biol. 7: 1057–1065.

Tan, L. and Mort, A. (2020). Extensins at the front line of plant defence. A commentary on: 'Extensin arabinosylation is involved in root response to elicitors and limits oomycete colonization'. Ann. Bot. 125: VII–VIII.

Velasquez, S.M. et al. (2015). Low sugar is not always good: Impact of specific o-glycan defects on tip growth in arabidopsis. Plant Physiol. 168: 808–813.

Velasquez, S.M. et al. (2011). O-Glycosylated Cell Wall Proteins Are Essential in Root Hair Growth. Science (80-.). 332: 1401–1403.

Voxeur, A., Wang, Y., and Sibout, R. (2015). Lignification: Different mechanisms for a versatile polymer. Curr. Opin. Plant Biol. 23: 83–90.

Weigel, D. and Mott, R. (2009). The 1001 genomes project for Arabidopsis thaliana. Genome Biol. 10: 107.

Xu, C., Zhao, L., Pan, X., and Šamaj, J. (2011). Developmental localization and methylesterification of pectin epitopes during somatic embryogenesis of banana (Musa spp. AAA). PLoS One 6.

van Zelm, E., Zhang, Y., and Testerink, C. (2020). Salt Tolerance Mechanisms of Plants. Annu. Rev. Plant Biol. 71: 403–433.

Zou, Y., Zhang, Y., and Testerink, C. (2022). Root dynamic growth strategies in response to salinity. Plant. Cell Environ. 45: 695–704.